

Analysis of seismic anisotropy parameters for sedimentary strata

Fuyong Yan¹, De-Hua Han¹, Samik Sil², and Xue-Lian Chen³

ABSTRACT

Based on a large quantity of laboratory ultrasonic measurement data of sedimentary rocks and using Monte Carlo simulation and Backus averaging, we have analyzed the layering effects on seismic anisotropy more realistically than in previous studies. The layering effects are studied for different types of rocks under different saturation conditions. If the sedimentary strata consist of only isotropic sedimentary layers and are brine-saturated, the δ value for the effective transversely isotropic (TI) medium is usually negative. The δ value will increase noticeably and can be mostly positive if the sedimentary strata are gas bearing. Based on simulation results, c_{13} can be determined by other TI elastic constants for a layered medium consisting of isotropic layers. Therefore, δ can be predicted from the other Thomsen parameters with confidence. The theoretical expression of δ for an effective TI medium consisting of isotropic sedimentary rocks can be simplified with excellent accuracy into a neat form. The anisotropic properties of the interbedding system of shales and isotropic sedimentary rocks are primarily influenced by the intrinsic anisotropy of shales. There are moderate to strong correlations among the Thomsen anisotropy parameters.

INTRODUCTION

At various scales, the earth and the subsurface are often modeled as a layered sequence of different constituents. Sedimentary strata are layered sedimentary rocks. Observed from the outcrops and seismic profiles, the most prominent feature of sedimentary basins is often their layered structure. The elastic properties of a layered medium can be described by transverse anisotropy (Postma, 1955; Anderson, 1961; Backus, 1962; Helbig, 1984).

At the low-frequency limit, i.e., when the wavelength is much greater than the layer thicknesses, the effective anisotropic properties of two periodically alternating isotropic layers are described by Postma (1955). Backus (1962) extends the model to any combination of layers with either isotropic or transversely isotropic (TI) properties. Schoenberg and Muir (1993) further extend the Backus model to more general cases where the constituent layers can be any type of anisotropic media. From the wireline-logging data, the lithology or acoustic property variations of the sedimentary layers are often in a scale of decimeters, whereas the wavelength of the seismic waves is usually approximately 100 m. Therefore, the effective media through which the seismic waves propagate are usually, more or less anisotropic. Study of the effective anisotropic properties of the layered media is important for seismic exploration.

The importance of seismic anisotropy on seismic imaging and seismic data interpretation is well-understood (Alkhalifah and Tsvankin, 1995; Helbig and Thomsen, 2005), but consideration of seismic anisotropy also puts great challenges on seismic data processing because extra parameters are introduced. In exploration geophysics, the seismic anisotropic properties are conveniently defined by the Thomsen (1986) parameters. Based on Backus averaging and Monte Carlo simulation of two- and three-layer cake models, Berryman (1999) analyzes the relationships among the Thomsen parameters. The study shows little indication of the correlations between the anisotropy parameters except for the possible range and sign of the parameters. The simulation results were not very helpful for understanding the seismic anisotropic properties of sedimentary rocks.

In Berryman's (1999) study, the elastic parameters for the layered model are assumed to have uniform distributions in certain ranges. This assumption may be far from true for sedimentary rocks. In this study, a more realistic study will be performed using similar approaches by Berryman (1999), but the Monte Carlo simulation will be based on a large quantity of laboratory measurement data of sedimentary rocks. More constituent layers with either isotropic or transversely anisotropic properties are included to simulate the complexity of sedimentary strata.

Manuscript received by the Editor 30 January 2016; revised manuscript received 10 April 2016; published online 11 July 2016.

¹University of Houston, Rock Physics Laboratory, Houston, Texas, USA. E-mail: yanfyon@yahoo.com; dhan@uh.edu.

²Occidental Petroleum, Houston, Texas, USA. E-mail: samiksil@gmail.com.

³China University of Petroleum, School of Geosciences, Qingdao, China. E-mail: chenxl@upc.edu.cn.

© 2016 Society of Exploration Geophysicists. All rights reserved.

MONTE CARLO SIMULATION OF SEDIMENTARY STRATA

In terms of volume fraction and lithology, the sedimentary formations primarily consist of mudstone, carbonate, and sandstone (Grotzinger and Jordan, 2010). The mudstone refers to clastic rocks with fine particles. The terms mudstone and shale are used interchangeably, and no distinction is made between them in this study. Carbonate and sandstone are usually very weak in elastic anisotropy and are assumed isotropic in this study. Shales are assumed intrinsically anisotropic by default. From the wireline logging data, the vertical lithological variations causing noticeable acoustic velocity change are often in the order of tens of centimeters or less, whereas the velocities of seismic waves

are determined by effective properties of the formation unit with a thickness of tens of meters. Therefore, to model the effective properties of the sedimentary layers, it would be more realistic to use multiple layers instead of two or three layers. For the wireline logging data, the S-wave velocity is often less reliable than the P-wave velocity information or it is often not acquired. It is very rare that the anisotropic parameters can be fully acquired from the wireline logging data. Therefore, the logging data are usually not sufficient for an up-scale study.

Instead, this study is based on a large amount of laboratory ultrasonic measurement data of various sedimentary rocks. The sandstone data come from Han (1986). The sandstone samples in Han's data set include typical sandstones coming from various places all over the world. The samples have wide ranges of clay content and porosity. They are measured at dry and fully brine-saturated states and at various pressure conditions. The carbonate rocks come from Rafavich et al. (1984), Kenter et al. (1997), Woodside et al. (1998), Assefa et al. (2003), and Fabricius et al. (2008). The carbonate samples in data sets by Rafavich et al. (1984), Assefa et al. (2003), and Fabricius et al. (2008) are measured on dry and fully brine-saturated states. The shale data come from Thomsen (1986), Johnston and Christensen (1995), Vernik and Liu (1997), Jakobsen and Johansen (2000), Wang (2002, shale and coal samples only), and Sone (2012; Sone and Zoback 2013). The saturation conditions of shales are complicated and not classified for analysis. The data points for the dry sandstones are 420, for wet sandstones are 420; for dry carbonates are 144, for wet carbonates are 298; and for shales are 137. Figure 1 shows the probability density functions of α_0 , the ratio of α_0^2/β_0^2 , and the Thomsen (1986) parameters of the experimental data of different types of sedimentary rocks. Here, α_0 and β_0 are the vertical P- and S-wave velocities, respectively. The Thomsen parameters (ϵ , γ , and δ) are all zero for isotropic rocks, and only distributions of the Thomsen parameters of shales are shown in Figure 1. The dry and wet sandstones are treated as different classifications of rocks because the effect of saturation on seismic anisotropy parameters is to be studied. It can be seen that different classifications of rocks have different distributions of α_0 and the ratios of α_0^2/β_0^2 . Most of the distributions are close to normal with different central values. The carbonate rocks, dry or wet, have a wider distribution of α_0 . The shales have a wider distribution of α_0^2/β_0^2 compared with other classifications of sedimentary rocks, which may be due to usually more complicated mineral composition of shales. In Berryman's (1999) study, only isotropic layers are considered. The Monte Carlo simulations are based on a uniform distribution of α_0 between 2.5 and 5.5 km/s and a uniform distribution of α_0^2/β_0^2 between 0.12 and 0.42. From Figure 1, it can be seen that the layer property parameterization in Berryman's (1999) study is not optimal for the sedimentary rocks.

In our study, sedimentary strata are simulated by first randomly selecting a certain number of samples from a classification of rocks or a combination of classifications of rocks, and then the experimental data of the selected samples are used to parameterize the layer cake model. The elastic properties of each layer in the layer cake model are based on laboratory measurement, not on random sampling in certain ranges that may lose the physical relations between the elastic parameters for the real sedimentary rocks. This is the basic difference between our study and the study by Berryman (1999). Considering the size of the database and the number of simulations, a 15-layer cake model is used. Compared with the two- or three-layer cake model, the 15-layer cake model may be more proper to simulate the complex subsurface conditions.

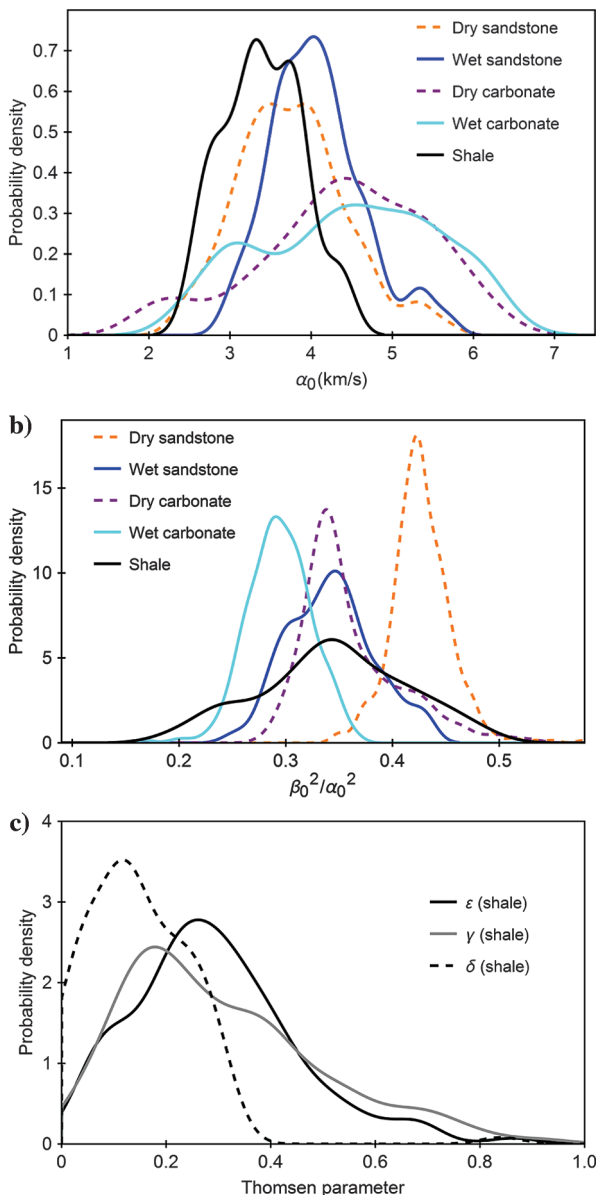


Figure 1. Probability densities of (a) α_0 , (b) β_0^2/α_0^2 , and (c) the Thomsen parameters of the laboratory data used in this study. In panel (c), only the Thomsen parameters of shales are shown because they are all zero for isotropic rocks.

BACKUS AVERAGING

The effective elastic properties of a material consisting of fine layers with isotropic or TI properties are transversely anisotropic. Backus (1962) brings up a model to estimate the effective anisotropic properties of a finely layered medium when the wavelength is much longer than the thicknesses of the individual layers. In Voigt notation, the five effective TI elastic constants are computed by

$$c_{11B} = \left\langle c_{11} - \frac{c_{13}^2}{c_{33}} \right\rangle + \left\langle \frac{c_{13}}{c_{33}} \right\rangle^2 \langle c_{33}^{-1} \rangle^{-1}, \quad (1)$$

$$c_{13B} = \left\langle \frac{c_{13}}{c_{33}} \right\rangle \langle c_{33}^{-1} \rangle^{-1}, \quad (2)$$

$$c_{33B} = \langle c_{33}^{-1} \rangle^{-1}, \quad (3)$$

$$c_{44B} = \langle c_{44}^{-1} \rangle^{-1}, \quad (4)$$

$$c_{66B} = \langle c_{66} \rangle, \quad (5)$$

$$\rho_B = \langle \rho \rangle, \quad (6)$$

where $\langle * \rangle$ is a volume averaging operator. Equation 4 is actually the Reuss bound of c_{44} values of all the constituent layers. Equation 5 is the Voigt bound of the c_{66} values of all the constituent layers. The subscript B in this study denotes that the effective property is estimated by the Backus averaging model. The Backus model is reduced to the Postma (1955) model when a material consists of only two periodically alternating isotropic layers. The Schoenberg and Muir (1989) model extended to the Backus model to a layered medium consisting of layers with arbitrary type of anisotropy. The Backus averaging model is sufficient for this study because only isotropic or TI layers are considered.

LAYERING EFFECT ON SEISMIC ANISOTROPY IN SEDIMENTARY STRATA OF A SINGLE LITHOLOGY

Due to mild depositional environment changes, for the same type of rocks, the mineral composition and texture variation may also cause noticeable acoustic velocity change. The layering effect on seismic anisotropy may be different for different classifications of rocks. The effects are studied by Monte Carlo simulation and Backus averaging. First, 15 samples are randomly selected from the experimental database for one of the five classifications of sedimentary rocks, and the corresponding experimental data are used to parameterize the 15-layer cake model. Backus averaging is applied to estimate the effective anisotropic properties of the sedimentary strata. For simplicity, each layer has the same thickness. Variation of the layer thickness is actually simulated even if an equal layer thickness model is used,

because a sample can be repeatedly selected and samples with similar properties may be selected. The order of parameterization of the 15-layer cake model does not matter because the Backus averaging model is used to compute the effective properties. For each classification of rocks, 5000 simulations are run.

Figures 2, 3, and 4 show the simulation results of the layering effect on seismic anisotropy. In Figure 2, for all the classifications

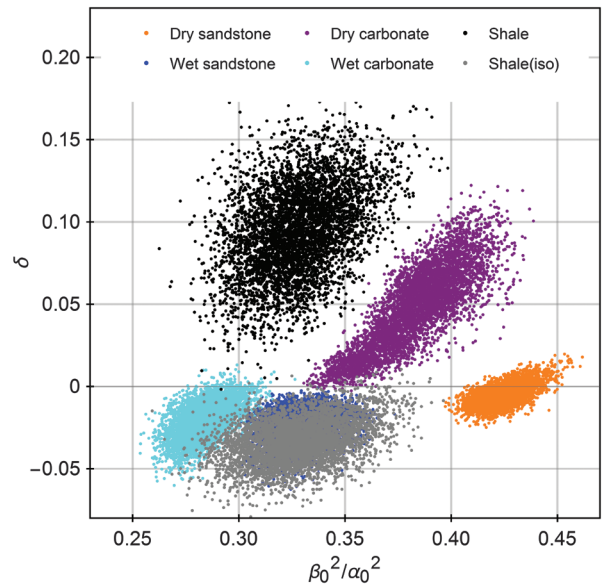


Figure 2. Crossplot between δ and β_0^2/α_0^2 . The δ and β_0^2/α_0^2 are computed from the Backus averaging of a 15-layer cake model randomly parameterized by the laboratory measurement data. Each cloud of points is from 5000 simulations. For the gray data points, the shale layer is assumed isotropic with the vertical properties.

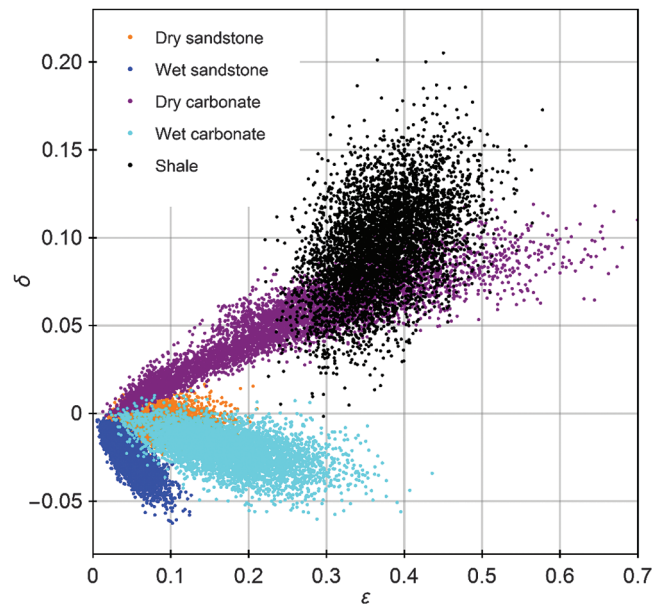


Figure 3. Crossplot between ϵ and δ . The ϵ and δ are computed from Backus averaging of a 15-layer cake model randomly parameterized by the laboratory measurement data. Each cloud of points is from 5000 simulations.

of rocks, the ratio α_0^2/β_0^2 has a noticeable effect on the δ value. Here, the gray data points are for the stratified shale formation with each layer assumed isotropic with the vertical properties. For the layered model of wet sandstones, wet carbonates, or isotropy-assumed shales, the δ values are usually negative. After considering the intrinsic anisotropic properties of the shale layers, the δ values are usually positive. The acoustic properties of gas-bearing rocks should be between the wet and dry rocks, but they should generally be closer to the dry rocks if the gas saturation is not too low. Therefore, gas saturation has an effect of increasing the δ value. Figure 3 shows the correlation between ε and δ for the five classifications of sedimentary rocks. It can be seen that for the wet sandstone and wet carbonate layers, ε is inversely correlated with δ , whereas for the dry carbonate rocks and shales, ε is positively correlated with δ . Quite different from Berryman's (1999) study, negative values of ε are not observed from 25,000 simulations. It is generally observed and accepted that the seismic velocity is greater along the bedding than in the perpendicular direction if the effect of fractures is not considered. Therefore, the simulation results in this study seem to be more realistic.

Figure 4 shows the correlation between ε and γ . The relations between the P- and S-wave anisotropies are different for different classifications of sedimentary rocks. Generally, the S-wave anisotropy is stronger than the P-wave anisotropy except for the gas-bearing carbonate layers. The ratio of S- to P-wave anisotropies will decrease due to the gas saturation effect. The ranges of P- and S-wave anisotropies for carbonate layers are greater than the sandstone layers simply because the experimental data for the carbonate rocks have wider distributions of acoustic properties, as can be seen from Figure 1. Comparing the correlations in Figures 2–4, the correlation between ε and γ is the strongest, especially for the isotropic layers of same lithology.

The rock samples for the experimental database come from different geologic units and depths; variation of the acoustic properties

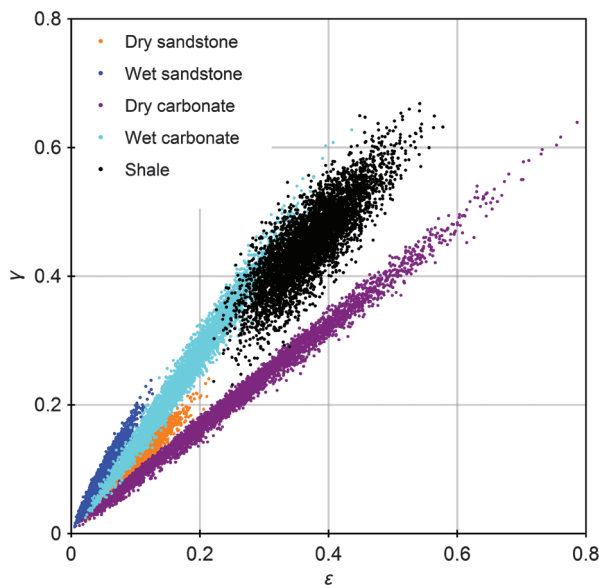


Figure 4. Crossplot between ε and γ . The ε and γ are computed from Backus averaging of a 15-layer cake model randomly parameterized by the laboratory measurement data. Each cloud of points is from 5000 simulations.

shown in Figure 1 should be much stronger than the real subsurface scenarios when the sedimentary strata in a certain depth interval are considered. Therefore, for the real sedimentary strata, the layering effect on seismic anisotropy should be less significant than the simulation results, but the relationship between the P- and S-wave anisotropies should still be true for different classifications of rocks. The simulation results are constrained by the distributions of the elastic properties of the laboratory database. The relationships may vary slightly for different areas.

PREDICTION OF δ FOR SEDIMENTARY STRATA CONSISTING OF ISOTROPIC LAYERS

At the low-frequency limit, the layered media can be treated as a TI medium defined by five elastic constants: c_{11} , c_{33} , c_{44} , c_{66} , and c_{13} . The physical meanings of c_{11} , c_{33} , c_{44} , and c_{66} are straightforward, and they can usually be reliably determined. The physical meaning of c_{13} is not obvious, and there are often significant uncertainties in the laboratory determination of c_{13} (Yan et al., 2012, 2013, 2014, 2015). Relations between the anisotropy parameters may be important for practical applications of seismic anisotropy. Therefore, it may be useful to find the correlations between c_{13} and other TI elastic constants.

Based on previous simulation results, Figure 5 shows the correlation between c_{13} and other TI elastic constants. It can be seen that c_{13} can almost perfectly be predicted by other TI elastic constants. The correlation formula is

$$c_{13B} = -0.048 + 0.48c_{11B} + 0.46c_{33B} - 0.53c_{44B} - 1.27c_{66B}. \quad (7)$$

The elastic constants are all in GPa, and the regression coefficient is 0.999 based on 20,000 simulations. Considering the different elastic properties between sandstone and carbonate, dry and wet rocks, the

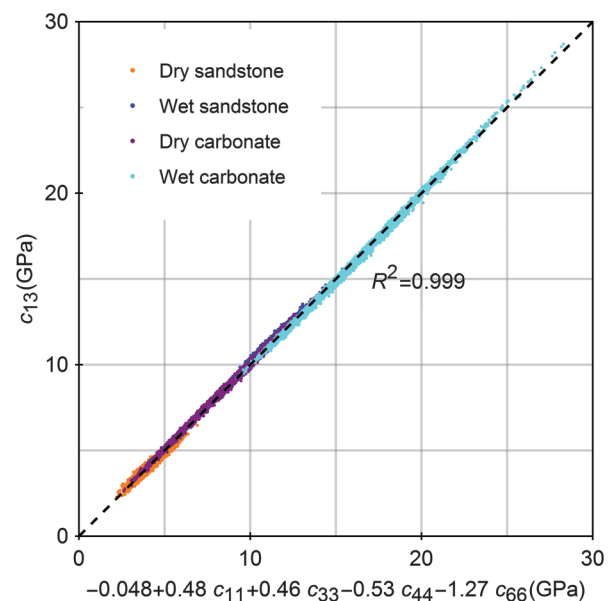


Figure 5. Relation between c_{13} and other TI elastic constants based on Backus averaging of a randomly selected 15-layer cake model. The 5000 simulations are run for each type of rocks.

high-degree correlation is not expected. This means that the elastic properties of a TI medium consisting of isotropic layers can be determined by four independent elastic constants (and not five as for a general TI medium). This is similar to the case of TI anisotropy caused by horizontal cracks (Gueguen et al., 2011).

Compared with the c_{13} values of common sedimentary rocks, the constant term in equation 7 is negligible. After dropping the constant term, using definitions of the Thomsen parameters, equation 7 can be converted to

$$\delta = \frac{-(1-r_0^2)^2 + (0.455 + 0.466r_0^2 + 0.479(1+2\varepsilon_B) - 1.267r_0^2(1+2\gamma_B))^2}{2(1-r_0^2)} \tag{8}$$

where r_0 is the ratio of β_0/α_0 .

Figure 6 shows a comparison between δ computed by the Backus averaging and δ predicted by equation 8. The result is consistent with the previous study that δ can be predicted from the other Thomsen parameters (Yan et al., 2015).

It should be emphasized that equation 8 only works for sedimentary strata consisting of isotropic layers. As shown in Figure 7, if shale layers with intrinsic anisotropy are mixed up with isotropic layers, equation 8 will not work and will usually underestimate δ .

APPROXIMATION OF δ FOR SEDIMENTARY STRATA CONSISTING OF ISOTROPIC LAYERS

The Thomsen parameter δ is important for seismic data processing because it determines the relation between the vertical interval velocity and the NMO velocity. As Thomsen (1986) describes, δ is an “awkward” combination of the TI elastic constants and its physical meaning is ambiguous. From study of the Backus averaging of two and three isotropic layers, Berryman (1999) finds that

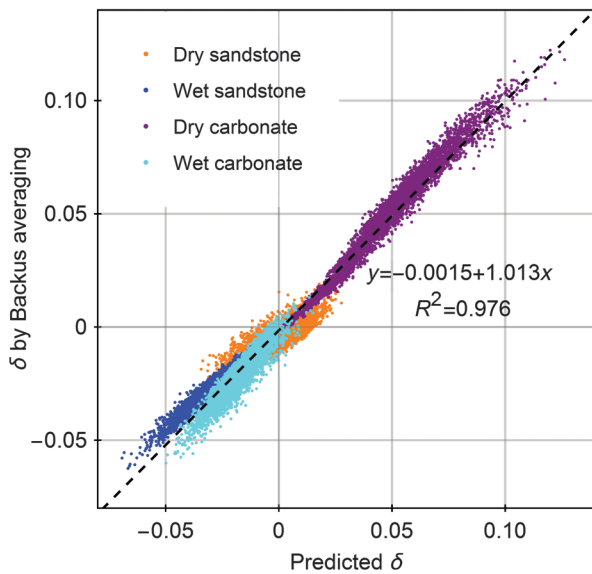


Figure 6. Prediction of δ from the other Thomsen parameters based on Backus averaging of randomly selected 15-layer cake model. The 5000 simulations are run for each type of rocks.

$$\text{Sign}(\delta_B) = \text{Sign}\left(\langle\alpha_0^{-2}\rangle - \langle\beta_0^{-2}\rangle\left\langle\frac{\beta_0^2}{\alpha_0^2}\right\rangle\right). \tag{9}$$

It would be nicer to rewrite the above equation in the following form:

$$\text{Sign}(\delta_B) = \text{Sign}\left(\frac{\langle\alpha_0^{-2}\rangle}{\langle\beta_0^{-2}\rangle} - \left\langle\frac{\beta_0^2}{\alpha_0^2}\right\rangle\right). \tag{10}$$

In this study, further exploration is made on the sign and the physical meaning of δ . From the definition of δ ,

$$\delta_B = \frac{(c_{13B} + c_{44B})^2 - (c_{33B} - c_{44B})^2}{2c_{33B}(c_{33B} - c_{44B})}. \tag{11}$$

Substituting equations 2–4 into the above equation and making further algebraic manipulations, we have

$$\delta_B = 2\left(\frac{\langle c_{44}^{-1} \rangle^{-1}}{\langle c_{33}^{-1} \rangle^{-1}} - \langle c_{44} \rangle\right) \frac{1 - \langle c_{44} \rangle}{1 - \frac{\langle c_{44}^{-1} \rangle^{-1}}{\langle c_{33}^{-1} \rangle^{-1}}}. \tag{12}$$

Here, $\langle c_{44}^{-1} \rangle^{-1}$ is the Reuss bound of c_{44} values and $\langle c_{33}^{-1} \rangle^{-1}$ is the Reuss bound of the c_{33} values. The ratio of $\langle c_{44}^{-1} \rangle^{-1}$ to $\langle c_{33}^{-1} \rangle^{-1}$ should be less than one. It is obvious that the rightmost term in the above equation should always be positive for natural rocks; therefore,

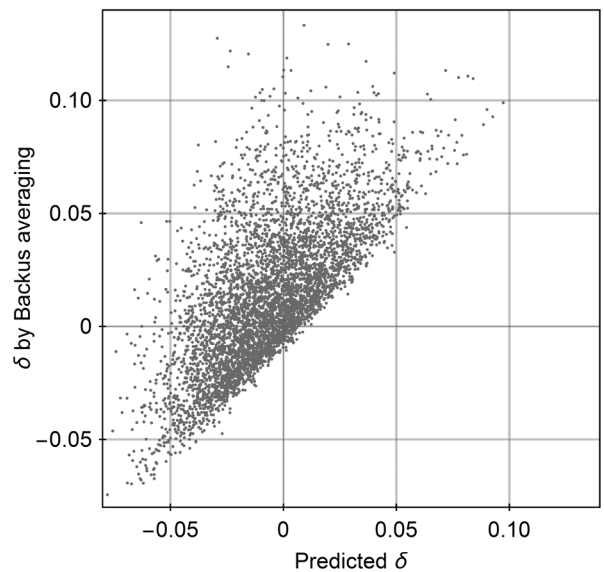


Figure 7. Prediction of δ from the other Thomsen parameters based on Backus averaging of a 15-layer cake model. The elastic properties of the 15-layer cake model are randomly selected from mixture of dry and wet sandstones, dry and wet carbonates and shale, and each classification of rocks has 20% chance to be selected. The value of δ is predicted using equation 8.

$$\text{Sign}(\delta_B) = \text{Sign}\left(\left\langle\frac{c_{44}^{-1}}{c_{33}^{-1}}\right\rangle^{-1} - \left\langle\frac{c_{44}}{c_{33}}\right\rangle\right). \quad (13)$$

Equation 13 is a more accurate expression than equation 10 because there is no assumption of constant densities. The sign of δ is determined by the difference between two types of c_{44}/c_{33} ratios computed by different approaches: one approach is to calculate the ratio of the Reuss bound of c_{44} to the Reuss bound of c_{33} . The other approach is to calculate the Voigt bound of the c_{44}/c_{33} ratios of the constituent layers.

From Monte Carlo simulation of sedimentary strata consisting of isotropic layers, as shown in Figure 8, the ratio of $(1 - \langle c_{44}/c_{33} \rangle)$ to $(1 - [\langle c_{44}^{-1} \rangle^{-1} / \langle c_{33}^{-1} \rangle^{-1}])$ is generally very close to one. Therefore, for sedimentary strata consisting of isotropic layers, equation 12 can be simplified into

$$\delta = 2\left(\left\langle\frac{c_{44}^{-1}}{c_{33}^{-1}}\right\rangle^{-1} - \left\langle\frac{c_{44}}{c_{33}}\right\rangle\right). \quad (14)$$

Figure 9 shows a comparison between δ calculated by the Backus averaging and δ approximated by equation 14 based on Monte Carlo simulation of sedimentary strata consisting of isotropic layers. The difference between the theoretical δ and the approximated δ values is only noticeable at extremely low and high δ values.

LAYERING EFFECT ON SEISMIC ANISOTROPY FOR SEDIMENTARY STRATA OF MIXED LITHOLOGIES

Except for mild acoustic property change caused by the mineral composition and texture variation for the same type of sedimentary rocks, stronger acoustic property change in a sedimentary formation can be caused by a drastic depositional environment change leading to a lithology change. For example, the interbedding of shales with sandstones and interbedding of shales with carbonate rocks are

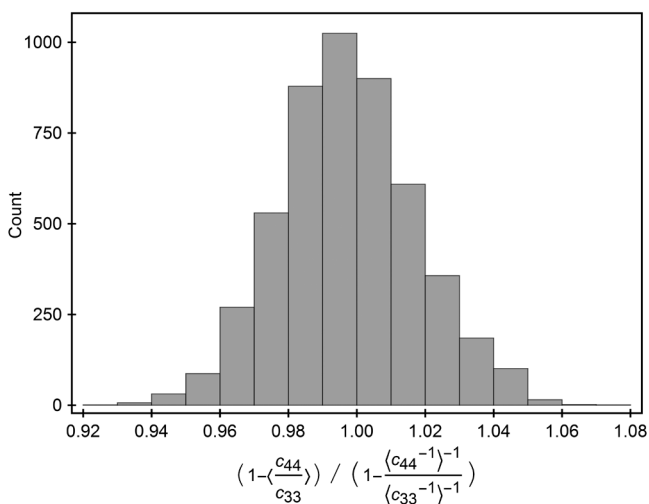


Figure 8. Distribution of $(1 - \langle c_{44}/c_{33} \rangle) / (1 - \langle c_{44}^{-1} \rangle^{-1} / \langle c_{33}^{-1} \rangle^{-1})$ from a 15-layer cake model randomly selected from the laboratory data of dry or wet sandstones and dry or wet carbonates. Totally 5000 simulations are run.

often-occurring geologic scenarios. To model the interbedding effect on seismic anisotropy, the 15-layer cake model is randomly parameterized by the experimental database of shales and one classification of the isotropic rocks. Figure 10 shows an example of Monte Carlo simulation of the sedimentary strata consisting of shale and dry sandstone layers. There are 30 realizations of the 15-layer cake model. Some realizations may have more shale layers and some realizations may have more sandstone layers, but each layer has an equal chance to be shale or the dry sandstone layer. When lithology for each layer is determined, a sample from the corresponding experimental database is randomly selected to parameterize the layer properties. For each combination of shale with the other classification of isotropic rocks, 5000 simulations are run.

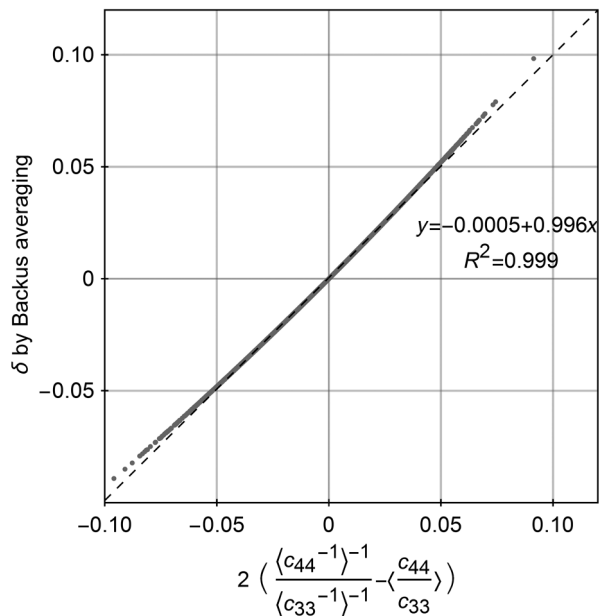


Figure 9. Prediction of δ by $2([\langle c_{44}^{-1} \rangle^{-1} / \langle c_{33}^{-1} \rangle^{-1}] - \langle c_{44}/c_{33} \rangle)$ based on a 15-layer cake model randomly selected from the laboratory data of dry or wet sandstone and dry or wet carbonate. Totally, 5000 simulations are run.

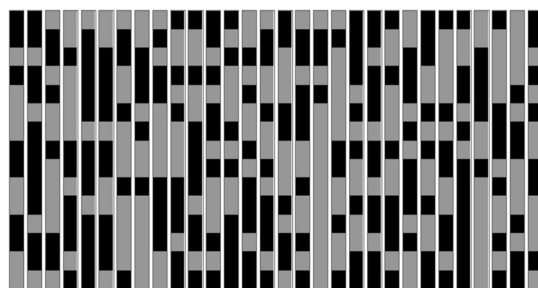


Figure 10. Monte Carlo simulation of the random interbedding between shales (black) and dry sandstone (gray) layers. Each column represents one of the 30 realizations of the 15-layer cake model. Each layer has same thickness and an equal chance to be shales or dry sandstone layer. The elastic properties of the constituent layers of the same lithology are randomly selected from the corresponding experimental database, and they are usually different from each other.

Figures 11, 12, and 13 show the simulation results of the interbedding effect on seismic anisotropy parameters. Comparing Figures 2–4 with Figures 11–13, if we know the layering effect on seismic anisotropy for each classification of the sedimentary rocks, the interbedding effect by two classifications of sedimentary rocks on seismic anisotropy is generally predictable. In Figure 11, when

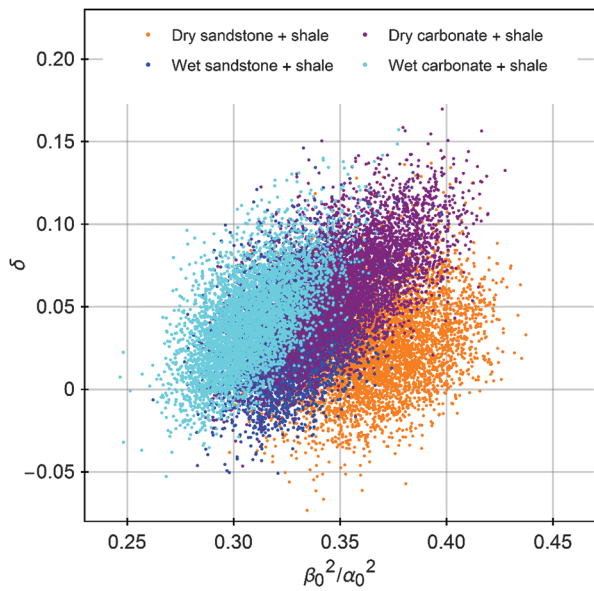


Figure 11. Crossplot between δ and β_0^2/α_0^2 . The δ and β_0^2/α_0^2 are computed from Backus averaging of a 15-layer cake model randomly parameterized by the laboratory measurement data. Each cloud of points is from 5000 simulations. Different colors represent mixtures of shale with different classifications of rocks.

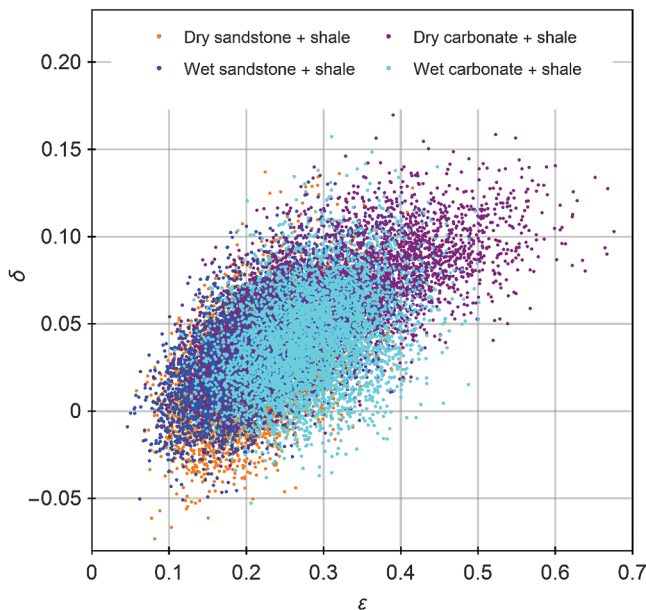


Figure 12. Crossplot between ϵ and δ . The ϵ and δ are computed from Backus averaging of a 15-layer cake model randomly parameterized by the laboratory measurement data. Each cloud of points is from 5000 simulations. Different colors represent mixture of shale with different classifications of rocks.

the intrinsic anisotropy of shales is considered, the δ values are mostly positive. In Figure 12, generally, there is a fair correlation between ϵ and δ . It can be seen from Figure 13 that there is a good correlation between ϵ and γ . Shales are a type of rock with complicated mineral composition including clay minerals, quartz and carbonate, and organic materials. The distributions of the anisotropic parameters of the interbedding systems are closer to those of shales than the isotropic layers; therefore, the anisotropic properties of the interbedding system are primarily influenced by the intrinsic anisotropy of shale layers. The interbedding effect on seismic anisotropy is in general consistent with the laboratory studies on shales (Sayers, 2005; Sondergeld and Chandra, 2011). Because the Monte Carlo simulation is based on the experimental data of real sedimentary rocks, the simulation results on the relationships among the seismic anisotropy parameters are quite different from those from Berryman’s (1999) study.

DISCUSSION

The Postma model can be treated as a special part of the Backus (1962) model, and the Schoenberg and Muir (1993) model is an extension of the Backus model. All these stress-strain average models for layered media assume infinitely fine layers and a “welded contact” between the layers (Schoenberg and Muir, 1989). For a two-layer medium consisting of two isotropic layers, if the two layers have drastically different elastic properties, it may not be proper to apply the above stress-strain average models because averaging of stresses or strains of the two layers may violate the rigid boundary assumption.

Many negative values of ϵ are found in Berryman’s (1999) simulation study. The physical meaning of negative ϵ is that the seismic velocity is slower in direction along the bedding than perpendicular to the bedding. This is in contradiction to common sense, but it is theoretically possible. Let us consider a two-layer cake model: The

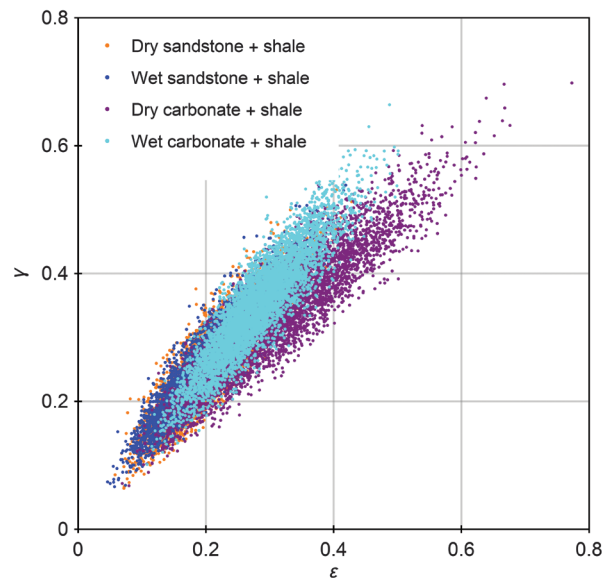


Figure 13. Crossplot between ϵ and γ . The ϵ and γ are computed from Backus averaging of a 15-layer cake model randomly parameterized by the laboratory measurement data. Each cloud of points is from 5000 simulations. Different colors represent mixture of shales with different classifications of isotropic rocks.

volume fraction of layer 1 is f_{1V} , and the volume fraction of layer 2 is $1 - f_{1V}$; the two layers have equal c_{33} , but different c_{44} (c_{441} for layer 1 and c_{442} for layer 2). According to Backus averaging, we have

$$c_{11B} = c_{33} - \frac{4(c_{441} - c_{442})^2(1 - f_{1V})f_{1V}}{c_{33}}, \quad (15)$$

$$c_{33B} = c_{33}. \quad (16)$$

It is obvious from the above equations that as long as the two layers do not have equal c_{44} , then $c_{11B} < c_{33B}$ and the effective ϵ will be negative. We analyze that negative ϵ rarely exists for the sedimentary strata because there is usually a positive correlation between c_{33} and c_{44} , i.e., the vertical P- and S-wave velocities. From our simulations study, when the number of layers is more than five, the probability of negative ϵ is close to zero. More studies may be needed to understand the applicability of these stress-strain average models.

CONCLUSION

Based on Backus averaging and Monte Carlo simulation, it is found that the δ value for the sedimentary strata consisting of isotropic wet sandstones or carbonates is usually negative and the gas-bearing thin beds have the effect of increasing the δ value. When intrinsic anisotropy of shales is considered, the δ value is usually positive. For sedimentary strata consisting of isotropic layers, the TI elastic constant c_{13} can be determined by other TI elastic constants and δ can be predicted from the other Thomsen parameters with good confidence. A simplified expression of δ with clear physical meaning is derived for the effective TI medium consisting of isotropic layers. The anisotropic properties of the interbedding system of shales and isotropic sedimentary rocks are primarily influenced by the intrinsic anisotropy of shales. There are moderate to strong correlations among the Thomson anisotropy parameters.

ACKNOWLEDGMENTS

We thank the Fluid/DHI Consortium sponsors for financial support. We also thank P. Dutta, O. Bokhonk, and an anonymous reviewer for their thorough review and constructive suggestions.

REFERENCES

Alkhalifah, T., and I. Tsvankin, 1995, Velocity analysis for transversely isotropic media: *Geophysics*, **60**, 1550–1566, doi: [10.1190/1.1443888](https://doi.org/10.1190/1.1443888).
 Anderson, D. L., 1961, Elastic wave propagation in layered anisotropic media: *Journal of Geophysical Research*, **66**, 2953–2963, doi: [10.1029/JZ066i009p02953](https://doi.org/10.1029/JZ066i009p02953).
 Assefa, S., C. McCann, and J. Southcott, 2003, Velocities of compressional and shear waves in limestones: *Geophysical Prospecting*, **51**, 1–13, doi: [10.1046/j.1365-2478.2003.00349.x](https://doi.org/10.1046/j.1365-2478.2003.00349.x).

Backus, G. E., 1962, Long-wave elastic anisotropy produced by horizontal layering: *Journal of Geophysical Research*, **67**, 4427–4440, doi: [10.1029/JZ067i011p04427](https://doi.org/10.1029/JZ067i011p04427).
 Berryman, J. G., 1999, Analysis of Thomsen parameters for finely layered VTI media: *Geophysical Prospecting*, **47**, 959–978, doi: [10.1046/j.1365-2478.1999.00163.x](https://doi.org/10.1046/j.1365-2478.1999.00163.x).
 Fabricius, I., L. Gommessen, A. Krogsboll, and D. Olsen, 2008, Chalk porosity and sonic velocity versus burial depth: Influence of fluid pressure hydrocarbons and mineralogy: *The American Association of Petroleum Geologists Bulletin*, **92**, 201–223, doi: [10.1306/10170707077](https://doi.org/10.1306/10170707077).
 Gueguen, Y., and M. Kachanov, 2011, Effective elastic properties of cracked and porous rock, in Y. M. Leroy, and F. K. Lehner, eds., *Mechanics of crustal rocks*, CISM courses: Springer, 533.
 Grotzinger, J., and T. H. Jordan, 2010, *Understanding earth*, 6th ed., W.H. Freeman.
 Han, D.-H., 1986, Effects of porosity and clay content on acoustic properties of sandstones and consolidated sediments: Ph.D. thesis, Stanford University.
 Helbig, K., 1984, Anisotropy and dispersion in periodically layered media: *Geophysics*, **49**, 364–373, doi: [10.1190/1.1441672](https://doi.org/10.1190/1.1441672).
 Helbig, K., and L. Thomsen, 2005, 75-plus years of anisotropy in exploration and reservoir seismic: A historical review of concepts and methods: *Geophysics*, **70**, no. 6, 9ND–23ND, doi: [10.1190/1.2122407](https://doi.org/10.1190/1.2122407).
 Jakobsen, M., and T. A. Johansen, 2000, Anisotropic approximation for mudrocks: A seismic laboratory study: *Geophysics*, **65**, 1711–1725, doi: [10.1190/1.1444856](https://doi.org/10.1190/1.1444856).
 Johnston, J. E., and N. I. Christensen, 1995, Seismic anisotropy of shales: *Journal of Geophysical Research*, **100**, 5591–6003.
 Kenter, J., F. Podladchikov, M. Reinders, S. van der Gaast, B. Fouke, and M. Sonnenfeld, 1997, Parameters controlling sonic velocities in a mixed carbonate-siliciclastic Permian shelf-margin (upper San Andres Formation, Last Chance Canyon, New Mexico): *Geophysics*, **62**, 505–520, doi: [10.1190/1.1444161](https://doi.org/10.1190/1.1444161).
 Postma, G. W., 1955, Wave propagation in a stratified medium: *Geophysics*, **20**, 780–806, doi: [10.1190/1.1438187](https://doi.org/10.1190/1.1438187).
 Rafavich, F., C. Kendall, and T. Todd, 1984, The relationship between properties and the petrographic character of carbonate rocks: *Geophysics*, **49**, 1622–1636, doi: [10.1190/1.1441570](https://doi.org/10.1190/1.1441570).
 Sayers, C. M., 2005, Seismic anisotropy of shales: *Geophysical Prospecting*, **53**, 667–676, doi: [10.1111/gpr.2005.53.issue-5](https://doi.org/10.1111/gpr.2005.53.issue-5).
 Schoenberg, M., and F. Muir, 1993, A calculus for finely layered anisotropic media: *Geophysics*, **54**, 581–589, doi: [10.1190/1.1442685](https://doi.org/10.1190/1.1442685).
 Sondergeld, C. H., and S. R. Chandra, 2011, Elastic anisotropy of shales: *The Leading Edge*, **2011**, 325–331.
 Sone, H., 2012, Mechanical properties of shale gas reservoir rocks and its relation to in-situ stress variation observed in shale gas reservoirs: Ph.D. thesis, Stanford University.
 Sone, H., and M. D. Zoback, 2013, Mechanical properties of shale gas reservoir rocks — Part 1: Static and dynamic elastic properties and anisotropy: *Geophysics*, **78**, 5, D381–D392, doi: [10.1190/geo2013-0050.1](https://doi.org/10.1190/geo2013-0050.1).
 Thomsen, L., 1986, Weak elastic anisotropy: *Geophysics*, **51**, 1954–1966, doi: [10.1190/1.1442051](https://doi.org/10.1190/1.1442051).
 Vernik, L., and X. Liu, 1997, Velocity anisotropy in shales: A petrophysical study: *Geophysics*, **62**, 521–532, doi: [10.1190/1.1444162](https://doi.org/10.1190/1.1444162).
 Wang, Z., 2002, Seismic anisotropy in sedimentary rocks. Part 2: Laboratory data: *Geophysics*, **67**, 1423–1440, doi: [10.1190/1.1512743](https://doi.org/10.1190/1.1512743).
 Woodside, J., J. Kenter, and A. Köhnen, 1998, Acoustic properties from logs and discrete measurements (sites 966 and 967) on Eratosthenes Seamount: Controls and ground truth, in A. H. F. Robertson, K.-C. Emeis, C. Richter, and A. Camerlenghi, eds., *Proceedings of the Ocean Drilling Program: Scientific Results*, **160**, 535–543.
 Yan, F., D.-H. Han, and Q. Yao, 2012, Oil shale anisotropy measurement and sensitivity analysis: 82nd Annual International Meeting, SEG, Expanded Abstracts, 1–5.
 Yan, F., D.-H. Han, and Q. Yao, 2013, Physical constraints on c_{13} and Thomsen parameter delta for VTI rocks: 83rd Annual International Meeting, SEG, Expanded Abstracts, 2889–2894.
 Yan, F., D.-H. Han, and Q. Yao, 2014, Benchtop rotational group velocity measurement on shales: 84th Annual International Meeting, SEG, Expanded Abstracts, 2983–2986.
 Yan, F., D.-H. Han, and Q. Yao, 2015, Physical constraints on c_{13} and δ for transversely isotropic hydrocarbon source rocks: *Geophysical Prospecting*, **57**, 393–411, doi: [10.1111/1365-2478.12265](https://doi.org/10.1111/1365-2478.12265).